Gas Processing Journal

Vol. 6, No. 2, 2018, pp. 49-60
http://gpj.ui.ac.ir

DOI: http:// 10.22108/gpj.2019.113741.1044

The Effect of Sodium and Chloride Salts on Tetrahydrofuran Hydrate Formation by Using a Differential Scanning Calorimetry

Parisa Naeiji [1], Farshad Varaminian [2*]

[1,2] *Faculty of Chemical, gas and petroleum Engineering, Semnan University, Semnan, Iran*

Received: 2018-11-01 Revised: 2019-07-02 Accepted: 2019-07-13

Abstract: In this study, a differential scanning calorimetry (DSC) has been used to characterize tetrahydrofuran (THF) hydrate formation with and without the presence of sodium and chloride salts. The thermal properties including the heat of formation, phase change temperature and specific heat capacity of THF hydrate formation have been determined. When salts are present, THF hydrate is inhibited, so that the phase change temperature shifts to a lower temperature, a broadening of the DSC peak can be seen and the height of the peak and the heat of formation decreases. Because the heat capacity depends on the heat of formation, it reduces when salt is present. The results show that the sodium salt solutions have exhibited the best performance on delaying nucleation of hydrate in order of Na_2SO_3 > NaF > NaCl, while chloride salt solutions, especially $CaCl_2$, have demonstrated that can reduce the heat of formation to around 65% compared to that of without salt.

keywords: Tetrahydrofuran Hydrate; Differential Scanning Calorimetry; Formation Heat; Phase Change Temperature; Specific Heat Capacity

1. Introduction

Clathrate hydrates are inclusion compounds in which small guest molecules are captured in water cavities made up of hydrogen-bonded water molecules. Typical guest molecules include methane, ethane, carbon dioxide and some liquids that are stabilized in the cavities of sI, sII and sH hydrate via van der Waals interaction forces (Carroll, 2002; Erfani and Varaminian, 2017; Giavarini and Hester, 2011; Naeiji and Varaminian, 2013; Sloan, 2003; Sloan and Koh, 2008; Sun et al, 2011). Clathrate hydrates can be formed at low temperatures close to the freezing point of water and at high pressures that are also common in oil and gas transmission (Carroll, 2002; Mohebbi and Behbahani, 2014; Sloan, 2003; Sun et al, 2011; Vysniauskus and Bishnoi, 1983). Gas hydrates have been extensively investigated because of their importance in the petroleum industry especially because they are a major possible reason of pipeline blockage during the transport of gas or petroleum (Ellison et al., 2000; Hammerschmidt, 1934; Holder and Bishnoi, 2000; Karimi et al., 2014; Ng and Robinson, 1994).

Numerous techniques have been employed to investigate gas hydrates (Chazallon et al., 2007; Makogon, 1997). NMR and Raman spectroscopy are usually applied to characterize the gas hydrates (Chazallon et al., 2007; Kini and Sloan, 2002; Rovetto et al., 2008; Sum et al., 1997). Ripmeester and Ratcliffe (1990) have developed an NMR technique to assess the clathrate hydrate forming ability of new potential guest molecules and to determine their structure. Also, Gupta et al. (2007) have studied the methane hydrate dissociation mechanism on the molecular scale using NMR spectroscopy. They found a relationship between NMR methane gas chemical shift, pressure, and temperature of the system (Gupta et al., 2007). Hydrate properties, such as structure and composition have been measured using Raman spectroscopy reported by Hester et al. (2007). Moreover, Susilo et al. (2007) have synthesized and characterized structure I and H methane hydrate with PXRD, NMR, Raman spectroscopy and DSC.

Differential Scanning Calorimetry (DSC) is one of the most common techniques of thermal analysis of Physico-chemical transformation that it consists of monitoring the heat

* Corresponding Author.
Authors' Email Address: [1] P. Naeiji (parisa.naieji@gmail.com), [2] F. Varaminian (fvaraminian@semnan.ac.ir)

ISSN (Online): 2345-4172, ISSN (Print): 2322-3251

exchange between the sample and a reference. It has been used to study hydrates since 1980 (Giavarini and Hester, 2011). This has proved to be a valuable technique in the investigation of gas hydrate formation and dissociation. Dalmazzone et al. (2003) have been presented experiments using DSC to determine the thermodynamic equilibrium properties of methane hydrate in complex solutions. Lachance et al. (2008) have studied the effect of gas hydrate formation/dissociation on water-in-oil emulsions stability using DSC. In addition, it has been used to evaluate hydrate nucleation and kinetic hydrate inhibitor performance trends (McNamee, 2011).

It has been previously found that some liquids such as furan, tetrahydrofuran (THF) and 1,4-dioxane are non-gaseous hydrate former that they can form sII hydrate under atmospheric pressure (Chun and Lee, 2000; Ding et al., 2010; Dirdal et al., 2012; Erfani et al., 2015; Erfani and Varaminian, 2016; Gough and Davidson, 1971; Karamoddin and Varaminian, 2013, 2014a, 2014b; Naeiji et al., 2014a, 2014b). They can be used as suitable alternative molecules to study the gas hydrates without the requirement of highpressure equipment. On the other hand, their formation heat is comparable to the fusion heat of ice, so that they can be considered as suitable alternative materials in air-conditioning systems (Fournaison et al., 2004; Li et al., 2006; Mahmoudi et al., 2016a, 2016b; Marinhas et al., 2006). THF is a cyclic ether completely miscible with water that can form hydrate at 4 ˚C and atmospheric pressure (Karamoddin and Varaminian, 2014a; Naeiji et al., 2014a). DSC analysis has been also employed to determine the thermal properties and enthalpy of THF hydrate formation by Zhang et al. (2004). Hydrate formation conditions of water-THF-CO_2 systems have been investigated by DSC to show the effect of THF on equilibrium pressure and dissociation enthalpy of CO_2 hydrate applied to secondary refrigeration (Delahaye et al., 2006). Li et al. (2010, 2012, and 2013) have also widely studied on the hydrates as cold storage materials by using DSC. They have obtained the phase change temperature and fusion heat of tetra-*n*-butyl ammonium bromide (TBAB) and THF hydrate (Li et al., 2010).

In this study, it is tried to evaluate THF hydrate formation by the DSC technique. It has been previously reported by Parlouër et al. (2004) that additives influence the methane hydrate formation so that the introduction of sodium chloride and ethylene glycol allows to shift the dissociation temperature obtained from DSC at a higher value for a significative pressure. Similarly, Koh et al. (1998) have also used DSC to test hydrates inhibitors at atmospheric pressure. Consequently, the thermal properties including the heat of formation, phase change temperature and specific heat capacity of THF hydrate formation in the presence of sodium and chloride salts have been determined.

2. Experimental Method

2.1. Materials

The samples have been made using freshly deionized and distilled water, and tetrahydrofuran liquid (purity: 99.5 vol%) provided by the Merck company. The salts used are sodium chloride, sodium fluoride, sodium sulfite, potassium chloride and calcium chloride with a normal purity of 99.5% (Merck Co.).

2.2. Apparatus and Procedure

A DSC setup has been used in this study (see Figure 1). The experimental system consisted of two cylindrical stainless steel cells (about 1 cm^3) placed into a copper segment. This segment includes three rectangular cube form sub-segments, so that sample and reference cells placed into the middle segment. The heating/cooling process is conducted by peltier effect, so that a 4×4 (cm×cm) peltier is in direct contact with the middle segment on the one side and with the lateral copper segment on another side. Input and output streams of refrigerant fluid (ethylene glycol solution-50 mol%) provided by a refrigerated circulator is inserted into the lateral copper segment to reduce the temperature of the hot surface of peltier. The copper segment placed into a plexiglass chamber which has been isolated by perlite granules and vacuum. Two platinum thermometers (Pt 100) with temperature accuracy of ±0.01 ˚C have been placed under each of the cells to monitor/control the temperature of the calorimeter. The temperature of the calorimetry is controlled through a temperature program with a cooling rate of 0.5 ˚C.min^{-1}.

For the test, a sample of 0.5±0.025 cc of the water-THF solution along with salt at the concentrations of 0.1-1 wt% has been prepared. THF forms structure II hydrate in the molar composition of THF.$17H_2O$ at atmospheric condition ($P \approx 1$ atm and low temperatures) (Naeiji et al., 2014a). The equation of the hydration reaction is as follows (Karamoddin and Varaminian, 2014a):

$$THF + 17H_2O \rightarrow THF.17H_2O + Q \quad (1)$$

where Q is the heat of formation since THF hydrate formation is an exothermic process. The prepared sample has been injected into the sample cell. The reference cell has been prepared in the same way as the sample cell but without the sample. Then, the sample and reference cells have been placed in the specified cavities. The temperature ramp method (Hohne et al., 2003) has been used to cool the sample from 10 to -5 °C at 0.5 °C.min^{-1}. The runs have been repeated two or three times to observe the results repeatability.

It should be noticed that the calibration runs have to perform before the main experimental runs. In this work, the calibration runs were done based on the freezing/melting temperature and heat of fusion of ice, corresponding more closely with the experimental temperature range. Since the heat capacity of ice, C, and heating/cooling rate, β, is available, the true heat flow can be determined by (Hohne et al., 2003):

$$C.\beta = \Phi_{true} = K_{\Phi}.\Phi_m$$

where Φ and K_{Φ} are the measured heat flow and the calibration factor, respectively. In the DSC, the measurement signal, ΔT, is obtained as electric voltage (with temperature accuracy of ±0.01 °C). The measured heat flow, Φ_m, is assigned to this signal by:

$$\Phi_m = -K.\Delta T$$

where K is given by the heat conduction path properties between the furnace and the sample. This factor was calculated by two decimals. The heat flow rate is also reported with two decimals so that its accuracy is 0.1 mW. Generally, the standard error of the value obtained from the DSC setup was around ±0.2-0.7.

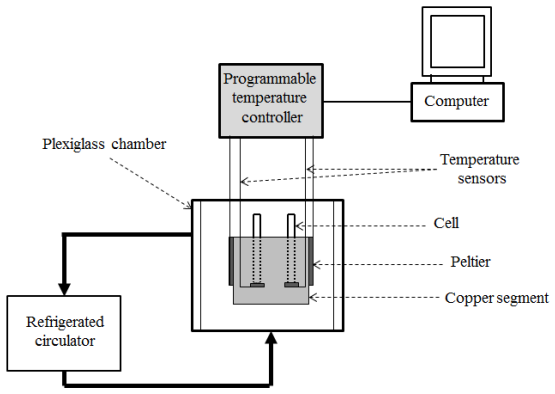

Figure 1. Schematic diagram of the experimental apparatus of DSC.

3. Results and Discussion

The ramp method has been used to measure the thermal properties of THF hydrate formation with or without the presence of sodium and chloride salts. As previously mentioned, the temperature and heat calibration has been performed based on the thermophysical properties of ice. The DSC curve of pure ice is shown in Figure 2. Only one exothermic peak observes in the heat flow curve for only the single substance (ice) under the process of freezing by DSC. The phase change temperature of ice investigated by DSC is 273.05±0.20 K that the deviation is only ±0.10 K compared with the standard value of ice (273.15 K). According to Figure 2, the temperature of peak and heat of formation corresponding to the peak area of pure ice have been determined to be 271.84±0.22 K and 164.01±0.21 J respectively. So, the deviation for the heat of formation is 5.53 J/g compared with the standard value (333.55 J/g).

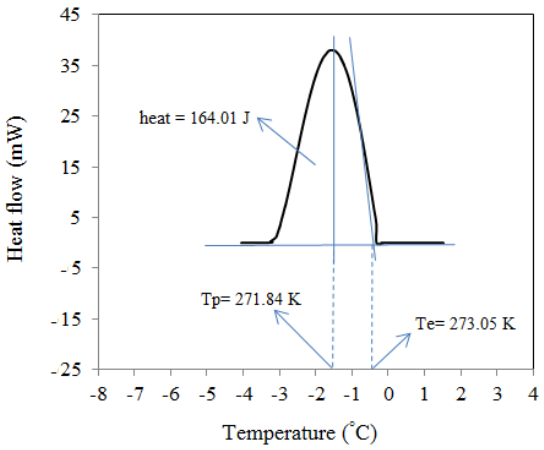

Figure 2. DSC freezing curve of ice.
(Tp: temperature of peak, Te: phase change temperature)

The DSC curve of THF hydrate formation is given in Figure 3. With regard to the THF hydrate, the phase change temperature is 276.36 K. Since THF and water are also mutually soluble, it is also easily explained by the fact that the phase change temperature is lower than the critical formation temperature point (277.55 K) in the THF hydrate phase equilibrium diagram (Sloan and Koh, 2008). The heat of formation that equals the enthalpy of formation is 66.15±0.47 J or 132.30 J/g that is comparable with that of reported in the literature (Li et al., 2010). Figure 4 shows the DSC curve of THF hydrate formation in the presence of sodium chloride at various concentrations (0.1-1 wt%). The results are

also given in Table 1. It is observed that THF hydrate is inhibited in the presence of NaClso that the DSC peak shifts to lower temperature. In other words, a delay in the phase change temperature occurs, so that it approximately shifts to 272.30 K in 1.0 wt% NaCl solution. Besides, a broadening of the DSC peak can be seen, however the height of peak decreases. The results are shown in Table 1 also confirm that the heat of formation decreases in the presence of NaCl and more decreases by adding NaCl. The r_Q represents the reduction percent of formation heat of salt solution compared to that of without salt. Increasing this criterion reveals that salt solution can inhibit THF hydrate formation so that 1.0 wt% NaCl solution with r_Q of 41.35% represents the highest ability in the inhibition performance.

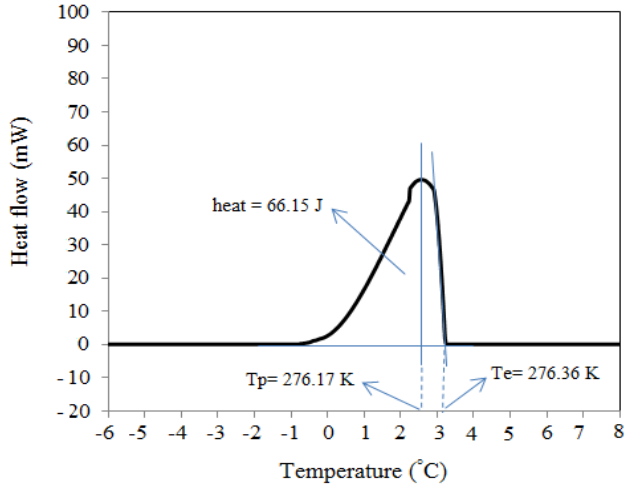

Figure 3. DSC curve of THF hydrate formation. (Tp: temperature of peak, Te: phase change temperature)

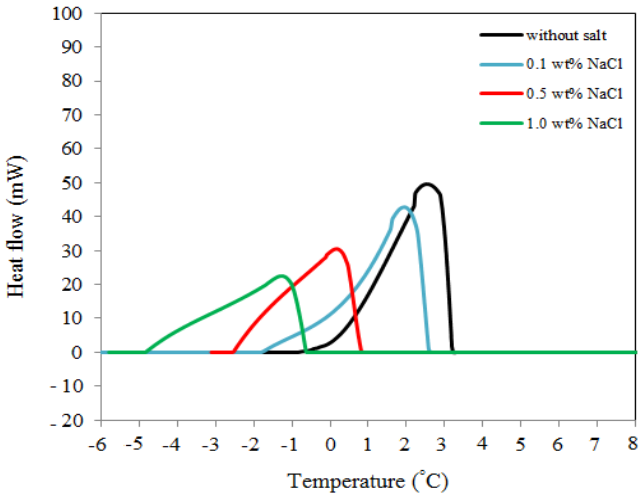

Figure 4. DSC curve of THF hydrate formation at various NaCl concentrations.

Table 1. The results of THF hydrate formation in the presence of NaCl.

System	T_e (K)[a]	T_p (K)[b]	Q (J)[c]	r_Q (%)[d]
Without salt	276.36 ± 0.25 [e]	276.17 ± 0.24 [e]	66.15 ± 0.47 [e]	
0.1 wt% NaCl	276.07 ± 0.29	274.93 ± 0.25	50.40 ± 0.19	23.81 ± 0.59 [e]
0.5 wt% NaCl	273.84 ± 0.36	273.20 ± 0.31	44.06 ± 0.35	33.39 ± 0.25
1.0 wt% NaCl	272.30 ± 0.22	271.82 ± 0.22	38.79 ± 0.25	41.35 ± 0.47

(a) T_e: phase change temperature, (b) T_p: temperature of peak, (c) Q: formation heat, (d) r_Q: reduction percent of formation heat of salt solution compared to that of without salt, and (e) standard error.

The DSC curve of THF hydrate formation in the presence of sodium fluoride at various concentrations is represented in Figure 5. When NaF is added to the solution, the hydrate formation is postponed and the phase change temperature shifts from 276.36 K of without salt to 270.76 K of 1.0 wt% NaF aqueous solution. Similar to the NaCl solutions, it is clear that the height of peaks decreases and their widths is extended. So, it is to be expected the hydrate growth occurs slow. According to Table 2, the heat of formation of NaF solutions is lower than that of without salt. The criterion of r_Q represents a reduction of 7.80-31.43%.

Figure 6 and Table 3 are given the results of DSC for Na_2SO_3 solutions. It is found that Na_2SO_3 can also act on the nucleation of THF hydrate, since it shifts the phase change temperature from 276.36 K of without salt to 270.87 K of 0.1 wt% Na_2SO_3 aqueous solutions, and decreases the heat flow rate. Contrary to NaCl and NaF solutions, an increase in the salt concentration causes an increase in the formation of heat and a decrease in r_Q criterion. So that the solution of 0.1 wt% Na_2SO_3 represents a reduction of 56.68% in the formation heat compared to that of without salt. It means that the inhibition performance of hydrate formation is weakened when the salt concentration increases. It is likely related to the fact that heavier salt may be precipitated as the hydrate formation proceeds.

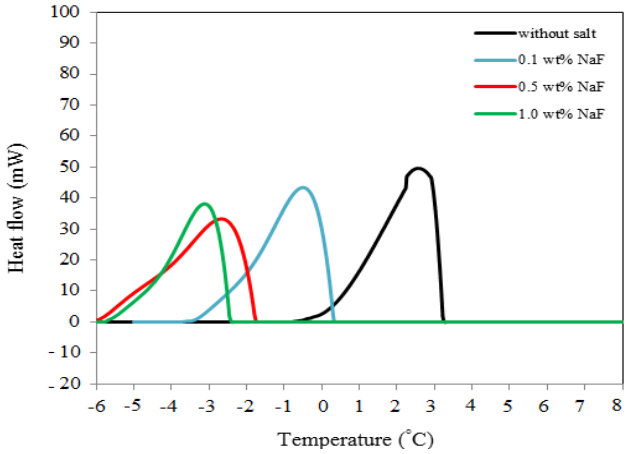

Figure 5. DSC curve of THF hydrate formation at various NaF concentrations.

Table 2. The results of THF hydrate formation in the presence of NaF.

System	T_e (K)[a]	T_p (K)[b]	Q (J)[c]	r_Q (%)[d]
Without salt	276.36 ± 0.25[e]	276.17 ± 0.24[e]	66.15 ± 0.47[e]	
0.1 wt% NaF	273.36 ± 0.26	272.32 ± 0.29	60.99 ± 0.34	7.80 ± 0.27[e]
0.5 wt% NaF	271.51 ± 0.34	270.56 ± 0.32	56.89 ± 0.28	13.99 ± 0.41
1.0 wt% NaF	270.76 ± 0.44	270.40 ± 0.42	45.36 ± 0.44	31.43 ± 0.06

(a) T_e: phase change temperature, (b) T_p: temperature of peak, (c) Q: formation heat, (d) r_Q: reduction percent of formation heat of salt solution compared to that of without salt, and (e) standard error.

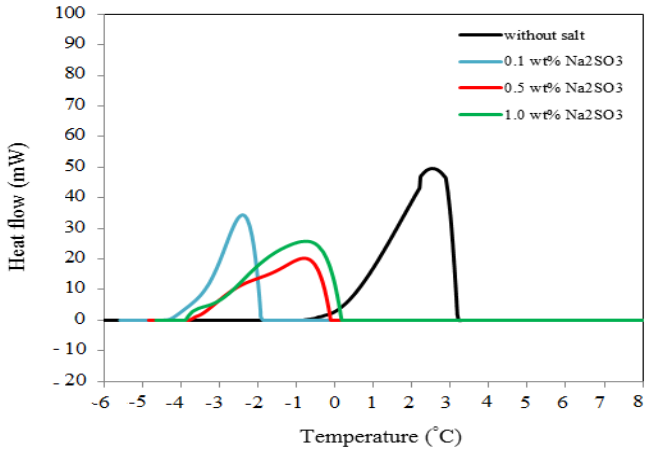

Figure 6. DSC curve of THF hydrate formation at various Na2SO3 concentrations.

Table 3. The results of THF hydrate formation in the presence of Na2SO3.

System	T_e (K)[a]	T_p (K)[b]	Q (J)[c]	r_Q (%)[d]
Without salt	276.36 ± 0.25 [e]	276.17 ± 0.24 [e]	66.15 ± 0.47 [e]	
0.1 wt% Na_2SO_3	270.87 ± 0.19	270.85 ± 0.18	28.73 ± 0.24	56.68 ± 0.48 [e]
0.5 wt% Na_2SO_3	272.97 ± 0.26	272.27 ± 0.25	32.83 ± 0.31	50.37 ± 0.34
1.0 wt% Na_2SO_3	273.79 ± 0.25	271.86 ± 0.27	46.14 ± 0.36	30.24 ± 0.23

(a) T_e: phase change temperature, (b) T_p: temperature of peak, (c) Q: formation heat, (d) r_Q: reduction percent of formation heat of salt solution compared to that of without salt, and (e) standard error.

The results obtained from THF hydrate formation in the presence of potassium chloride and calcium chloride is represented in Figs. 7-8 and Table 4-5. Both chloride salts can postpone the hydrate formation and decrease the heat flow rate. It is clear that the phase change temperature shifts from 276.36 K of without salt to 271.74 K and 273.79 at 1.0 wt% potassium chloride and 0.1 wt% calcium chloride salt aqueous solutions, respectively. The criterion of r_Q has a maximum value of 56.28% at 1.0 wt% KCl solution, while it reduces as the concentration of $CaCl_2$ into the solution increases.

Comparison of sodium and chloride salts shows that they can influence both nucleation and growth of THF hydrate formation. It has been previously proved that electrolytes (salts) as additives disrupt hydrogen bonding in water and the freezing point of water is lowered, so that ice is no longer stable at 273.15 K and one can vary the amount of freezing point depression achieved based on the additive chosen (Giavarini and Hester, 2011). This change can be considered to predict hydrate formation condition like ice. Salts affect hydrate formation as thermodynamic inhibitors and decrease the stable hydrate temperature for a given pressure (Barduhn et al., 1962; Chun and Lee, 2000; Englezos and Bishnoi, 1988; Kubota et al., 1984).

The results show different performances of salts on the inhibition of THF hydrate formation. The salt solutions of NaF and Na_2SO_3 have exhibited the best performance on delaying nucleation of the hydrate. These salts can postpone the hydrate formation by lowering the phase change temperature from 276.36 K to about 270 K. On the contrary, KCl and $CaCl_2$ solutions have demonstrated that can reduce the heat of formation to around 65% compared to that of without salt. It can be explained by the fact that the dual moment of the clathrate of hydrate is theoretically zero and they are neutral. But, they are experimentally biased because the water protons locate irregularly at hydrate cages so that it causes a partial positive charge temporary assigns for each cage. Consequently, anions of salts are placed near the hydrate surface and can disrupt the hydrate clathrate, while cations of salts can prevent the accumulation of hydrate clusters in the growth stage. The anions of sodium salt solutions show a more effect on the disruption of water cages in the nucleation stage.

Park et al. (2011) have proved that the inhibition effect of salts on hydrate formation is directly related to the number of electrical charges, while it has an inverse relation to the ionic size. As seen in Tables 1-3, by comparing the temperature of peak and the phase change temperature, it is clear that the order of inhibition strength among chloride salts isNa_2SO_3 > NaF > NaCl. Also, the highest value of r_Q belongs to the Na_2SO_3 solution. Similarly, the inhibition effect of chloride salts on hydrate nucleation is: $CaCl_2$ > NaCl > KCl, as seen in Tables 1, 4 and 5. Also, the solution of $CaCl_2$ has the most reduction in the formation of heat compared to that of without salt. The obtained results are in agreement with the results reported by Karamoddin and Varaminian (2013). Moreover, the freezing point is one of the colligative properties of solutions that depend on the concentration of solute molecules or ions, and not on the type of chemical species (McQuarrie et al., 2011). The measurement of the difference between the freezing point of a pure solvent and that of a solution including some solutes is expressed as follows (McQuarrie et al., 2011):

$$\Delta T_f = T_f(solution) - T_f(solvent) = -k_f.m \quad (4)$$

where k_f is the freezing point depression constant and m is the molality. k_f is present for a well-known solvent like water, but it is unknown for THF hydrate formation process. So, it can be determined by reported data from DSC. Table 6 gives the freezing point depression constant, k_f, for sodium and chloride salt solutions. The large k_f implies that the given salt is an effective material for inhibiting hydrate formation. It can be found that the highest amount of the freezing point depression constant belongs to the solution of Na_2SO_3 and $CaCl_2$ among sodium and chloride salts, respectively.

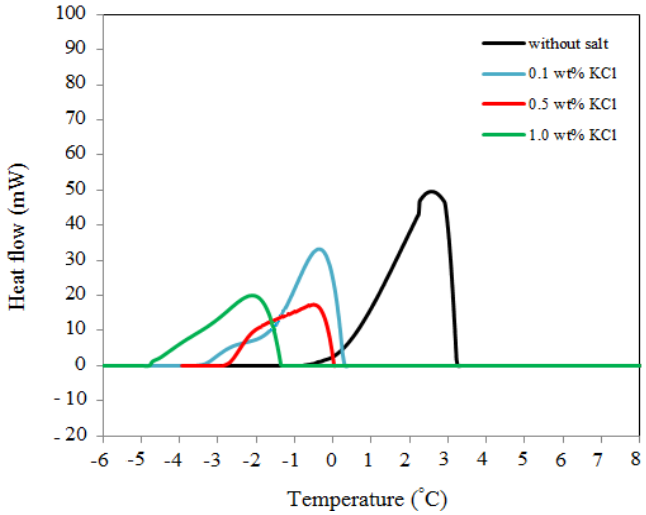

Figure 7. DSC curve of THF hydrate formation at various KCl concentrations.

Table 4. The results of THF hydrate formation in the presence of KCl.

System	T_e (K)[a]	T_p (K)[b]	Q (J)[c]	r_Q (%)[d]
Without salt	276.36 ± 0.25 [e]	276.17 ± 0.24 [e]	66.15 ± 0.47 [e]	
0.1 wt% KCl	273.71 ± 0.24	273.45 ± 0.27	39.69 ± 0.13	40.00 ± 0.72 [e]
0.5 wt% KCl	273.01 ± 0.29	272.40 ± 0.28	30.39 ± 0.25	54.06 ± 0.46
1.0 wt% KCl	271.74 ± 0.23	270.90 ± 0.25	28.92 ± 0.37	56.28 ± 0.21

(a) T_e: phase change temperature, (b) T_p: temperature of peak, (c) Q: formation heat, (d) r_Q: reduction percent of formation heat of salt solution compared to that of without salt, and (e) standard error.

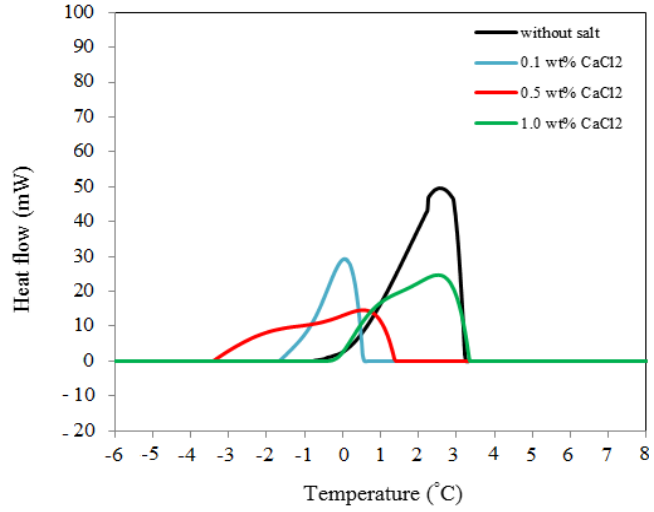

Figure 8. DSC curve of THF hydrate formation at various $CaCl_2$ concentrations.

Table 5. The results of THF hydrate formation in the presence of $CaCl_2$.

System	T_e (K)[a]	T_p (K)[b]	Q (J)[c]	r_Q (%)[d]
Without salt	276.36 ± 0.25 [e]	276.17 ± 0.24 [e]	66.15 ± 0.47 [e]	
0.1 wt% $CaCl_2$	273.79 ± 0.24	273.21 ± 0.29	24.13 ± 0.24	63.52 ± 0.48 [e]
0.5 wt% $CaCl_2$	274.89 ± 0.31	275.68 ± 0.18	32.79 ± 0.34	50.43 ± 0.27
1.0 wt% $CaCl_2$	276.48 ± 0.14	273.61 ± 0.32	43.11 ± 0.14	34.83 ± 0.71

(a) T_e: phase change temperature, (b) T_p: temperature of peak, (c) Q: formation heat, (d) r_Q: reduction percent of formation heat of salt solution compared to that of without salt, and (e) standard error.

Table 6. The freezing point depression constant, k_f, of THF hydrate formation.

System	Concen. wt%	ΔT_f	M (mol.Kg^{-1})	k_f (Kg.K.mol^{-1})
NaCl	0.1	0.29 ± 0.04 [a]	0.0171	16.95 ± 2.33 [a]
	0.5	3.82 ± 0.31	0.0856	44.65 ± 3.62
	1.0	2.26 ± 0.23	0.1711	13.21 ± 1.34
NaF	0.1	3.00 ± 0.25	0.0238	125.94 ± 10.50
	0.5	4.85 ± 0.29	0.1191	40.72 ± 2.43
	1.0	5.60 ± 0.34	0.2382	23.51 ± 1.42
Na_2SO_3	0.1	5.49 ± 0.22	0.0079	692.31 ± 27.84
	0.5	1.69 ± 0.15	0.0396	42.68 ± 3.78
	1.0	2.57 ± 0.25	0.0793	32.41 ± 3.15
KCl	0.1	2.65 ± 0.24	0.0134	197.76 ± 17.91
	0.5	2.07 ± 0.27	0.0671	30.85 ± 4.02
	1.0	1.62 ± 0.14	0.1341	12.08 ± 1.04
$CaCl_2$	0.1	2.57 ± 0.24	0.0090	285.56 ± 26.67
	0.5	1.20 ± 0.19	0.0451	26.61 ± 4.21
	1.0	1.47 ± 0.18	0.0901	16.32 ± 1.99

(a) standard error.

Heat capacity, or specific heat, is one of practical importance in the area of energy production such as hydrate formation. The heat capacity strongly depends on the heat of formation of the sample as follows:

$$C_p = \frac{dQ}{dT}$$

Limited researches have reported the heat capacity of hydrates (Sloan and Koh, 2008). The heat capacity of hydrates enhances with temperature and, it should be also measured under expected conditions. Handa (1986) has found that methane hydrate heat capacity linearly increases from 0.87 to 2.08 J.g^{-1}.K^{-1} between 85 and 270 K. Above the ice point from 279 to 285 K, Gupta et al. (2006) have reported that methane hydrate heat capacity increases from 2.08 to 2.28 J.g^{-1}.K^{-1}. These values are very similar to ice. Handa et al. (1984) have also determined the heat capacities of 0.841-2.097 J.g^{-1}.K^{-1} at 85-270 K for THF hydrate. In this work, the specific heat capacity of THF hydrate has been determined to be around 2.9 J.g^{-1}.K^{-1} at 276.17 K. When sodium salts are added, this value reduces to 2.64, 2.61 and 2.03 J.g^{-1}.K^{-1} for 0.1 wt% NaCl, NaF and Na_2SO_3 solutions, respectively. It agrees with the results obtained from Section 3.1. Since the order of inhibition strength among chloride salts is: Na_2SO_3 > NaF > NaCl, the lowest specific heat capacity is obtained from Na_2SO_3 solution. Moreover, the specific heat capacity of THF hydrate is determined to be 2.64, 1.96 and 1.80 J.g^{-1}.K^{-1} for 0.1 wt% NaCl, KCl and $CaCl_2$ solutions, respectively. Due to the heat flow rate dependency of the heat capacity, $CaCl_2$ solution shows the lowest specific heat capacity, according to the previous section.

4. Conclusions

In this work, THF hydrate formation in the presence of sodium and chloride salts has been studied using DSC. The results have been shown that sodium and chloride salts are effective in THF hydrate formation. When salt is present, THF hydrate is inhibited, so that the phase change temperature shifts to lower temperature. Moreover, a broadening of the DSC peak can be seen and the height of the peak and the heat of formation decreases. The sodium salt solutions have exhibited the best performance on delaying nucleation of hydrate in order of Na_2SO_3 > NaF > NaCl, while chloride salt solutions, especially $CaCl_2$, have demonstrated that can reduce the heat of formation to around 65% compared to that of without salt. Due to the heat flow rate dependency of the heat capacity, it reduces when salt is present, so that Na_2SO_3 and $CaCl_2$ solution shows the lowest specific heat capacity among the sodium and chloride salt solutions, respectively.

Nomenclature

C	Heat capacity
C_P	Specific heat capacity
H	Enthalpy
k_f	Freezing point depression constant
K	Inverse of heat conduction resistance between the furnace and the sample
K_Φ	Calibration factor
m	Molality
P	Pressure
Q	Heat of formation
r_Q	Reduction percent of formation heat

T	Temperature
T_e	Phase change temperature
T_f	Freezing point
T_p	Temperature of peak
wt%	Weight percent

Greek letters

β	Heating/cooling rate
Δ	Different operator
Φ_{true}	True heat flow
Φ_m	Measured heat flow

References

Barduhn, A.J., Towlson, H.E., Hu, Y.C., 1962. The properties of some new gas hydrates and their use in demineralizing sea water. A.I.Ch.E.J. 8, 176-183.

Carroll, J., 2002. Hydrate Types and Formers, Natural Gas Hydrate, Elsevier Science & Technology Books, pp. 19-30.

Chun, M.K., Lee, H., 2000. Phase Equilibria of R22 ($CHClF_2$) Hydrate Systems in the Presence of NaCl, KCl, and $MgCl_2$. J. Chem. Eng. Data 45, 1150–1153.

Chazallon, B., Focsa, C., Charlou, J.L., Bourry, C., Donval, J.P., 2007. A comparative Raman spectroscopic study of natural gas hydrates collected at different geological sites. Chem. Geol. 244, 175-185.

Dalmazzone, C., Herzhaft, B., Rousseau, L., Parlouer, P.L., Dalmazzone, D., 2003. Prediction of gas hydrates formation with DSC technique. Soc. Petrol. Eng. J. SPE 84315.

Delahaye, A., Fournaison, L., Marinhas, S., Chatti, I., 2006. Effect of THF on Equilibrium Pressure and Dissociation Enthalpy of CO_2 Hydrates Applied to Secondary Refrigeration. Ind. Eng. Chem. Res. 45, 391-397.

Ding, A., Wang, S., Pelemis, T., Crisafio, C., Lou, X., 2010. Specific critical concentrations of low dosage hydrate inhibitors in a THF–NaCl hydrate formation solution. Asia-Pac. J. Chem. Eng. 5, 577–584.

Dirdal, E.G., Arulanantham, C., Sefidroodi, H., Kelland, M.A., 2012. Can cyclopentane hydrate formation be used to rank the performance of kinetic hydrate inhibitors?. Chem. Eng. Sci. 82, 177–184.

Ellison, B.T., Gallagher, C.T., Frostman, L.M., Lorimer, S.E., 2000. The Physical Chemistry of Wax, Hydrates, and Asphaltene. Offshore Technology Conference, Houston, TX, OTC 11963.

Englezos, P., Bishnoi, P.R., 1988. Prediction of gas hydrate formation conditions in aqueous electrolyte solutions. A.I.Ch.E.J 34, 1718-1721.

Erfani, A., Taghizadeh, S., Karamoddin, M., Varaminian, F., 2015. Experimental and computational study on clathrate hydrate of tetrahydrofuran formation on a subcooled cylinder. Int. J. Refrig. 59, 84-90.

Erfani, A., Varaminian, F., 2016. Kinetic promotion of non-ionic surfactants on cyclopentane hydrate formation. J. Mol. Liq. 221, 963–971.

Erfani, A., Varaminian, F., 2017. Experimental investigation on structure H hydrates formation kinetics: Effects of surfactants on interfacial tension. J. Mol. Liq. 225, 636-644.

Fournaison, L., Delahaye, A., Chatti, I., Petitet, J.P., 2004. CO_2 hydrates in refrigeration processes. Ind. Eng. Chem. Res. 43, 6521-6526.

Giavarini, C., Hester, K., 2011. The Structure and Formation of Gas Hydrates, Physical Properties of Hydrates, Hydrates Seen as a Problem for the Oil and Gas Industry, Gas Hydrates, Immense Energy Potential and Environmental Challenges, Springer-Verlag, London, pp. 24, 25, 64, 104, 105.

Gough, S.R., Davidson, D.W., 1971. Composition of tetrahydrofuran hydrate and the effect of pressure on the decomposition. Can. J. Chem. 49, 2691-2699.

Gupta, A., Kneafsey, T.J., Moridis, G.J., Seol, Y., Kowalsky, M.B., Sloan, E.D., 2006. Composite thermal conductivity in a large heterogeneous porous methane hydrate sample. J. Phys. Chem. B 110, 16384-16392.

Gupta, A., Dec, S.F., Koh, C.A., Sloan, E.D., 2007. NMR Investigation of Methane Hydrate Dissociation. J. Phys. Chem. C 111, 2341-2346.

Hohne, G.W.H., Hemminger, W.F., Flammersheim H.-J., 2003. Differential scanning calorimetry, Springer-Veriag Berlin Heidelberg.

Hammerschmidt, E.G., 1934. Formation of Gas Hydrates in Natural Gas Transmission Lines. Ind. Eng. Chem. 26, 851–855.

Handa, Y.P., Hawkins, R.E., Murray, J.J., 1984. Enthalpies of fusion and heat capacities for ice and tetrahydrofuran (THF) hydrate in the range 85 to 270 K. J. Chem. Thermodynamics 16, 623-632.

Handa, Y.P., 1986. Compositions, enthalpies of dissociation, and heat capacities for clathrate hydrates of methane, ethane, and propane, and enthalpy of dissociation of isobutene hydrate, as determined by a heat-flow calorimeter. J. Chem. Thermodyn. 18, 915-921.

Holder, G.D., Bishnoi, P.R., 2000. Gas Hydrates, Challenges for the Future, New York.

Hester, K.C., Dunk, R.M., White, S.N., Brewer, P.G., Peltzer, E.T., Sloan, E.D., 2007. Gas hydrate measurements at Hydrate Ridge using Raman spectroscopy. Geochim. Cosmochim. Ac. 71, 2947-2959.

Karamoddin, M., Varaminian, F., 2013. Water desalination using R141b gas hydrate formation. Desalination and Water Treatment 1-7.

Karamoddin, M., Varaminian, F., 2014a. Performance of hydrate inhibitors in tetrahydrofuran hydrate formation by using measurement of electrical conductivity. J. Ind. Eng. Chem. 20, 3815-3820.

Karamoddin, M., Varaminian, F., 2014b. Study on the growth process of HCFC141b hydrate in isobaric system by a macroscopic kinetic model. Int. J. Refrig. 44, 66-72.

Karimi, R., Varaminian, F., Izadpanah, A.A., 2014. Study of ethane hydrate formation kinetics using the chemical affinity model with and without presence of surfactants. J. Non-Equilib. Thermodyn. 39, 219-229.

Kini, R.A., Sloan, E.D., 2002. Proceedings of the 4th International Conference on Gas Hydrates, Yokohama.

Koh, C.A., Westacott, R.E., Hirachand, K., Zugic, M., Zhang, W., Savidge, J.L., 1998. Proceeding 1998 Intern. Gas Research Conference, San Diego (USA) I, 194–200.

Kubota, H., Shimizu, K., Tanaka, Y., Makita, T., 1984. Thermodynamic properties of R13 (CClF3), R23 (CHF3), R152a (C2H4F2), and propane hydrates for desalination of sea water. J. Chem. Eng. Jpn. 17, 423-429.

Lachance, J.W., Sloan, E.D., Koh, C.A., 2008. Effect of hydrate formation/dissociation on emulsion stability using DSC and visual techniques. Chem. Eng. Sci. 63, 3942-3947.

Li, G., Liu, D., Xie, Y., 2010. Study on thermal properties of TBAB–THF hydrate mixture for cold storage by DSC. J. Therm. Anal. Calorim. 102, 819-826.

Li, G., Hwang, Y., Radermacher, R., 2012. Review of cold storage materials for air conditioning application. Int. J. Refrig. 35, 2053-2077.

Li, G., Hwang, Y., Radermacher, R., Chun, H.H., 2013. Review of cold storage materials for subzero applications, Energy 51, 1-17.

Li, J.P., Liang, D.Q., Guo, K.H., Wang, R.Z., Fan, S.S., 2006. Formation and dissociation of HFC134a gas hydrate in nano-copper suspension. Energ. Convers. Manage. 47, 201–210.

Mahmoudi, B., Naeiji, P., Varaminian, F., 2016a. Study of tetra-n-butylammonium bromide and tetrahydrofuran hydrate formation kinetics as a cold storage material for air conditioning system, J. Mol. Liq. 214, 96–100.

Mahmoudi, B., Naeiji, P., Varaminian, F., Mehdipour Ghazi, M., 2016b. Statistical optimization of hydrate formation conditions of TBAB and THF mixture as a cold storage material for air-conditioning system based on response surface methodology. Int. J. Refrigeration 69, 17-27.

Makogon, Y.F., 1997. Properties of hydrate, Hydrates of hydrocarbons, Penwell Books: Tulsa, pp. 91-106.

Marinhas, S., Delahaye, A., Fournaison, L., Dalmazzone, D., Fu¨rst, W., Petitet,

J.P., 2006. Modelling of the available latent heat of a CO_2 hydrate slurry in an experimental loop applied to secondary refrigeration. Chem. Eng. Process. 45, 184–92.

McNamee, K., 2011. Evaluation of hydrate nucleation trends and kinetic hydrate inhibitor performance by high-pressure differential scanning calorimetry. Proceedings of the 7th International Conference on Gas Hydrates (ICGH 2011), Edinburgh, Scotland, United Kingdom.

McQuarrie, D., Rock, P.A., Gallogly, E.B., 2011. Colligative properties of Solutions, General Chemistry, 4th Edition, Mill Valley: Library of Congress, pp. 44-46.

Mohebbi, V., Behbahani, R.M., 2014. Experimental study on gas hydrate formation from natural gas mixture. J. Nat. Gas Sci. Eng. 18, 47-52.

Naeiji, P., Varaminian, F., 2013. Experimental Study and Kinetics Modeling of Gas Hydrate Formation of Methane-Ethane Mixture. J. Non-Equilib. Thermodyn. 38, 273-286.

Naeiji, P., Arjomandi, A., Varaminian, F., 2014a. Amino acids as kinetic inhibitors for tetrahydrofuran hydrate formation: Experimental study and kinetic modeling. J. Nat. Gas Sci. Eng. 21, 64-70.

Naeiji, P., Arjomandi, A., Varaminian, F., 2014b. Optimization of inhibition conditions of tetrahydrofuran hydrate formation via the fractional factorial design methodology. J. Nat. Gas Sci. Eng. 21, 915-920.

Ng, H.J., Robinson, D.B., 1994. New Developments in the Measurement and Prediction of Hydrate Formation for Processing Needs. Ann. Acad. Sci. 715, 450–462.

Park, K.N., Hong, S.Y., Lee, J.W., Kang, K.C., Lee, Y.C., Ha, M.G., Lee, J.D., 2011. A new apparatus for seawater desalination by gas hydrate process and removal characteristics of dissolved minerals (Na+, Mg2+, Ca2+, K+, B3+), Desalination 274, 91-96.

Parlouër, P.L., Dalmazzone, C., Herzhaft, B., Rousseau, L., Mathonat, C., 2004. Characterisation of gas hydrates formation using a new high pressure micro-DSC. J. Therm. Anal. Calorim. 78, 165-172.

Ripmeester, J.A., Ratcliffe, C.I., 1990. ^{129}Xe NMR Studies of Clathrate Hydrates: New Guests for Structure II and Structure H. J. Phys. Chem. 94, 8773-8776.

Rovetto, L.J., Dec, S.F., Koh, C.A., Sloan, E.D., 2008. NMR studies on CH4+CO2 binary gas hydrates dissociation behavior. Proceedings of the 6th International Conference on Gas Hydrates (ICGH 2008), Vancouver, British Columbia, Canada.

Sloan, E.D., 2003. Clathrate hydrate measurements: microscopic, mesoscopic, and macroscopic. J. Chem. Thermodynamics 35, 41-35.

Sloan, E.D., Koh, C.A., 2008. Overview and Historical Perspective, Molecular Structures and Similarities to Ice, Hydrate Formation and Dissociation Processes, Clathrate Hydrates of Natural Gases, 3rd ed., Taylor & Francis–CRC Press, Boca Raton, FL, pp. 19, 20, 78-80, 94, 98, 119, 120, 140.

Sum, A.K., Burrus, R.C., Sloan, E.D., 1997. Measurement of clathrate hydrates via Raman spectroscopy. J. Phys. Chem. B, 101, 7371-7377.

Sun, C.Y., Li, W., Yang, X., Li, F., Yuan, Q., Mu, L., Chen, J., Liu, B., Chen, G.J., 2011. Progress in research of gas hydrate. Chin. J. Chem. Eng. 19, 151-162.

Susilo, R., Ripmeester, J.A., Englezos, P., 2007. Characterization of gas hydrates with PXRD, DSC, NMR, and Raman spectroscopy. Chem. Eng. Sci. 62, 3930-3939.

Vysniauskus, A., Bishnoi, P.R., 1983. A kinetics study of methane hydrate formation. Chem. Eng. Sci. 38, 1061.

Zhang, Y., Debenedetti, P.G., Prud'homme, R.K., Pethica, B.A., 2004. Differential Scanning Calorimetry Studies of Clathrate Hydrate Formation. J. Phys. Chem. B 108, 16717-16722.